

This article was downloaded by:

On: 25 January 2011

Access details: Access Details: Free Access

Publisher *Taylor & Francis*

Informa Ltd Registered in England and Wales Registered Number: 1072954 Registered office: Mortimer House, 37-41 Mortimer Street, London W1T 3JH, UK



## Separation Science and Technology

Publication details, including instructions for authors and subscription information:

<http://www.informaworld.com/smpp/title~content=t713708471>

### Extraction of Lanthanoids by Liquid Surfactant Membranes

Masaaki Teramoto<sup>a</sup>; Tadashi Sakuramoto<sup>a</sup>; Toru Koyama<sup>a</sup>; Hideto Matsuyama<sup>a</sup>; Yoshikazu Miyake<sup>a</sup>

<sup>a</sup> Department of Industrial Chemistry, Kyoto Institute of Technology Matsugasaki, Sakyo-Ku, Kyoto, Japan

**To cite this Article** Teramoto, Masaaki , Sakuramoto, Tadashi , Koyama, Toru , Matsuyama, Hideto and Miyake, Yoshikazu(1986) 'Extraction of Lanthanoids by Liquid Surfactant Membranes', Separation Science and Technology, 21: 3, 229 — 250

**To link to this Article:** DOI: 10.1080/01496398608058375

URL: <http://dx.doi.org/10.1080/01496398608058375>

## PLEASE SCROLL DOWN FOR ARTICLE

Full terms and conditions of use: <http://www.informaworld.com/terms-and-conditions-of-access.pdf>

This article may be used for research, teaching and private study purposes. Any substantial or systematic reproduction, re-distribution, re-selling, loan or sub-licensing, systematic supply or distribution in any form to anyone is expressly forbidden.

The publisher does not give any warranty express or implied or make any representation that the contents will be complete or accurate or up to date. The accuracy of any instructions, formulae and drug doses should be independently verified with primary sources. The publisher shall not be liable for any loss, actions, claims, proceedings, demand or costs or damages whatsoever or howsoever caused arising directly or indirectly in connection with or arising out of the use of this material.

## Extraction of Lanthanoids by Liquid Surfactant Membranes

MASAAKI TERAMOTO,\* TADASHI SAKURAMOTO,  
TORU KOYAMA, HIDETO MATSUYAMA, and  
YOSHIKAZU MIYAKE

DEPARTMENT OF INDUSTRIAL CHEMISTRY  
KYOTO INSTITUTE OF TECHNOLOGY  
MATSUGASAKI, SAKYO-KU, KYOTO 606, JAPAN

### Abstract

Separation and concentration of lanthanoids such as  $\text{La}^{3+}$ ,  $\text{Nd}^{3+}$ ,  $\text{Sm}^{3+}$ ,  $\text{Eu}^{3+}$ ,  $\text{Gd}^{3+}$ ,  $\text{Dy}^{3+}$ , and  $\text{Yb}^{3+}$  were carried out using liquid surfactant membranes containing 2-ethylhexyl phosphonic acid mono-2-ethylhexyl ester as a carrier. Under the condition of sufficiently high distribution ratio, more than 98% of these metal ions was extracted within 5 min even if the volume ratio of W/O emulsion to the external aqueous phase was as low as 1/32. The ratio of the concentration of metal ions in the internal aqueous phase to that in the external feed phase reached about 50,000 within 20 min. In the conventional solvent extraction of  $\text{Yb}^{3+}$ , the aggregates of metal-carrier complexes, which were insoluble in the organic membrane phase, were formed at high loading ratio. In the extraction of  $\text{Yb}^{3+}$  by liquid surfactant membranes, however, formation of such aggregates was suppressed because both extraction and stripping occurred simultaneously on both sides of the membranes. The rate of interfacial reaction between lanthanoids and the carrier was remarkably reduced by the presence of the emulsifier, and the forward reaction rate was represented by

$$r_f = k_f \{ \text{Ln}^{3+} \} [(\text{HR})_2]^3 / [\text{H}^+]^3$$

where  $[(\text{HR})_2]$  is the concentration of the dimer of the carrier. The rate of the extraction by liquid surfactant membranes was satisfactorily simulated by a proposed permeation model, i.e., a "multilayer shell model."

\*To whom correspondence should be addressed.

## INTRODUCTION

The separation technique using liquid surfactant membranes has been noted as a unique method for the separation and concentration of such solutes as metal ions, weak bases, weak acids, and amino acids (1). The most promising application among these is the concentration of metal ions by the active transport mechanism where carriers play important roles in fast and selective permeation. It was reported that various metal ions such as copper(II) (2), zinc(II) (3), chromium(IV) (4, 5), cobalt(II) (6), uranium(VI) (7), and mercury(II) (5) were successfully extracted by liquid surfactant membranes. However, very few papers (8, 9) were presented on the extraction of lanthanoids which are essential elements, especially in the electronic industries. Changyin et al. (8), and Yongjun et al. (9) carried out experiments on the extraction of  $\text{Eu}^{3+}$  and  $\text{La}^{3+}$  using liquid surfactant membranes containing di-2-ethylhexyl phosphoric acid as a carrier, and the data were simulated by the advancing front model (9). However, the resistances of the interfacial reactions and the diffusion of the metal ions in the external aqueous phase, which are often important depending on the experimental condition, were not considered in their model.

In order to discuss systematically the behavior of the extraction of lanthanoids, it is desirable to obtain experimental data on the extraction of a wide variety of lanthanoid ions. The purpose of the present study is to investigate the rate of permeation of such lanthanoid ions as  $\text{La}^{3+}$ ,  $\text{Nd}^{3+}$ ,  $\text{Sm}^{3+}$ ,  $\text{Eu}^{3+}$ ,  $\text{Gd}^{3+}$ ,  $\text{Dy}^{3+}$ , and  $\text{Yb}^{3+}$  by liquid surfactant membranes containing 2-ethylhexyl phosphonic acid mono-2-ethylhexyl ester (abbreviated as PC-88A) as a carrier. The distribution ratio of the metals and the kinetics of the interfacial reaction between the metals and the carrier were also investigated. The effect of the experimental conditions on the extraction rate was satisfactorily simulated by a new permeation model, i.e., the "multilayer shell model."

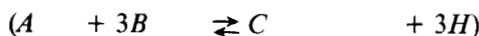
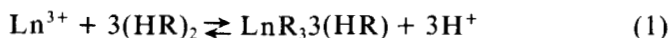
## MULTILAYER SHELL MODEL

The present authors earlier presented a model of the permeation of metal ions through liquid surfactant membranes by which the rates of both batch and continuous extractions of copper could be satisfactorily simulated (10, 11). Because the basic equations of the model are expressed by simultaneous partial differential equations, the integration is rather complicated. In the present study a simplified model, i.e., a

"multilayer shell model," is proposed. The computation time is considerably reduced by using this model.

The schematic diagram of the W/O emulsion drop is shown in Fig. 1. In this model the W/O emulsion drop is considered to consist of multilayer shells, each of which contains the oil membrane phase and the internal droplets. The mass transfer of the carrier and the complex occurs between adjacent shells, and the concentrations of the chemical species are uniform in each shell.

The reaction between lanthanoid ion (abbreviated as  $\text{Ln}^{3+}$ ) and PC-88A, and its equilibrium are expressed by the following equations (12):



$$K_{ex} = ([\text{LnR}_3(\text{HR})][\text{H}^+]^3 / [\text{Ln}^{3+}][(\text{HR})_2]^3)_{eq} = (CH^3/AB^3)_{eq} \quad (2)$$

Here,  $(\text{HR})_2$  is the dimer of PC-88A. As the solubility of PC-88A in the

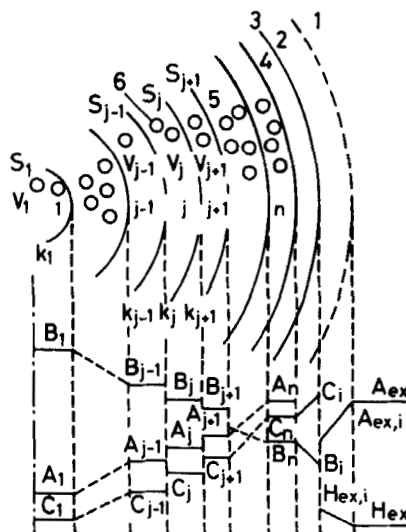


FIG. 1. Multilayer shell model. 1: External aqueous phase. 2: Stagnant film of the external aqueous phase outside W/O emulsion drop. 3: Interface between external aqueous phase and W/O emulsion drop. 4: Peripheral oil layer. 5: Oil membrane phase. 6: Internal aqueous phase.

aqueous phase is very low, it is deduced that the reaction occurs at the aqueous-organic interface. Here it is assumed that the reaction rate is represented by

$$\begin{aligned} r &= k_f([Ln^{3+}][(HR)_2]^3/[H^+]^3 - [LnR_3(HR)]/K_{ex}) \\ &= k_f(AB^3/H^3 - C/K_{ex}) \end{aligned} \quad (3)$$

where  $k_f$  is the forward reaction rate constant.

The elementary steps of the metal permeation are as follows.

- (1) Diffusions of  $Ln^{3+}$  and  $H^+$  through the stagnant film of the external aqueous phase.
- (2) Interfacial reaction between  $Ln^{3+}$  and the carrier.
- (3) Diffusions of the carrier and the complex through the peripheral oil layer of the W/O emulsion drop.
- (4) Diffusions of the carrier and the complex between the adjacent shells.
- (5) Stripping of the metal at the interface between the membrane phase and the internal aqueous phase.

The mass balance equation of  $Ln^{3+}$  in the external phase is represented by

$$(1 - \phi')(dA_{ex}/dt) = -k_A(S_T/V_T)(A_{ex} - A_{ex,i}) + (v_b/V_T)A_n \quad (4)$$

where  $k_A$  is the mass transfer coefficient of  $Ln^{3+}$  through the external stagnant film,  $S_T$  is the total external surface area of the W/O emulsion drops,  $V_T$  is the total volume of the W/O/W emulsion,  $\phi'$  is the volume fraction of the W/O emulsion drop ( $= V_o/V_T$ ), and  $v_b$  is the volumetric rate of the leakage of the internal aqueous phase to the external phase due to the breakage of the membranes. The last term of Eq. (4) represents the rate of the leakage of  $Ln^{3+}$  from the internal aqueous phase in the  $n$ th shell to the external phase (10).

The mass balance equations of the carrier  $B$  and the complex  $C$  in each shell are represented by

$$\begin{aligned} (1 - \phi)V_j(dB_j/dt) &= k_{B,j-1}S_{j-1}(B_{j-1} - B_j) - k_{B,j}S_j(B_j - B_{j+1}) \\ &+ (9\phi V_j/R_p)k_r(C_j - K_{ex}A_j B_j^3/H_j^3) \end{aligned} \quad (5)$$

$$\begin{aligned} (1 - \phi)V_j(dC_j/dt) &= k_{C,j-1}S_{j-1}(C_{j-1} - C_j) - k_{C,j}S_j(C_j - C_{j+1}) \\ &- (3\phi V_j/R_p)k_r(C_j - K_{ex}A_j B_j^3/H_j^3) \end{aligned} \quad (6)$$

$$V_j \phi (dA_j/dt) = (3\phi V_j/R_\mu) k_r (C_j - K_{ex} A_j B_j^3/H_j^3) \quad (7)$$

where  $k_r$  is the reverse reaction rate constant ( $= k_f/K_{ex}$ ). The above equations hold for  $i = 1, 2, \dots, n$ . Here,  $k_j$  is the mass transfer coefficient between the  $j$ th and the  $(j + 1)$ th shell. It should be noted that  $S_0$  is zero, and the  $(n + 1)$ th shell corresponds to the peripheral oil layer.

The initial conditions (I.C.) and the boundary conditions (B.C.) are as follows.

$$\begin{aligned} \text{I.C.: } A_{ex} &= A_{ex,0}, & B_j &= B_0, & C_j &= C_0, & A_j &= A_{in,0}, & (H_j &= H_{in,0}) \\ \text{at } t = 0, (j &= 1 - n) \end{aligned} \quad (8)$$

$$\begin{aligned} \text{B.C.: } k_A (A_{ex} - A_{ex,i}) &= k_H (H_{ex,i} - H_{ex})/3 = k_f (A_{ex,i} B_i^3/H_{ex,i}^3 - C_i/K_{ex}) \\ &= k_B (B_n - B_i)/3 = k_C (C_i - C_n) \end{aligned} \quad (9)$$

The charge balance equation in the internal aqueous phase is given by

$$3A_j + H_j = 3A_{in,0} + H_{in,0} \quad (10)$$

The way to divide the W/O emulsion drop into shells is important in this model. As the flux is closely related to the concentration profiles near the peripheral part of the W/O emulsion drop rather than those in the inner part, the division which results in thinner shells in the peripheral part for a given value of  $n$  is desirable. From this point of view, the drop was divided into shells of equal volume in this study. Then the following equations hold:

$$r_j = (j/n)^{1/3} R \quad (11)$$

$$S_j = 4\pi (j/n)^{2/3} R^2 \quad (12)$$

$$V_j = V_e/n = (4\pi/3)R^3/n \quad (13)$$

$$\Delta r_j = [(j/n)^{1/3} - \{(j - 1)/n\}^{1/3}]R \quad (14)$$

Here,  $r_j$  and  $\Delta r_j$  are the outer radius and the thickness of the  $j$ th shell, respectively. Mass transfer coefficients  $k_{B,j}$  and  $k_{C,j}$  are approximated by

$$\begin{aligned} k_{B,j} &= D_{e,B}/[(\Delta r_j + \Delta r_{j+1})/2] = (2D_{e,B}/R)/[\{(j + 1)/n\}^{1/3} \\ &\quad - \{(j - 1)/n\}^{1/3}] \end{aligned} \quad (15)$$

$$k_{C,j} = (2D_{e,C}/R)/[\{(j + 1)/n\}^{1/3} - \{(j - 1)/n\}^{1/3}] \quad (16)$$

where  $D_e$  is the effective diffusivity. The average thickness of the adjacent shells was taken as the diffusion length.

The basic equations are transformed to dimensionless forms by use of the variables and the parameters given by Eq. (24).

$$dy/d\theta = -\{3Bi\phi'/(1 - \phi')\}(y - y_i) + [aBim_{H,in}/\{2m_{A,ex}(1 - \phi')\}]a_n \quad (17)$$

$$db_i/d\theta = [3/\{(1 - \phi)v_j\}][\kappa_{B,j-1}s_{j-1}(b_{j-1} - b_j) - \kappa_{B,j}s_j(b_j - b_{j+1})] + \{3\phi qBi/(1 - \phi)\}z_j \quad (18)$$

$$dc_j/d\theta = [3r_{CB}/\{(1 - \phi)v_j\}][\kappa_{C,j-1}s_{j-1}(c_{j-1} - c_j) - \kappa_{C,j}s_j(c_j - c_{j+1})] - \{3\phi qBi/(1 - \phi)\}z_j \quad (19)$$

$$da_j/d\theta = (3Biq/m_{H,in})z_j \quad (20)$$

$$z_j = c_j - K_{ex}a_jb_j^3/\{m_{H,in}^2(1 + m_{A,in}/m_{H,in} - a_j)^3\} \quad (21)$$

$$\text{I.C.: } y = 1, \quad a_j = a_0 = 3A_{in,0}/H_{in,0}, \quad b_j = 1, \quad c_j = c_0 \\ = 3C_0/B_0 \text{ at } \theta = 0 \quad (22)$$

$$\text{B.C.: } y - y_i = (n_H m_{H,ex}/3m_{A,ex})(H_{ex,i}/H_{ex} - 1) \\ = n_j\{(y_i b_i^3/m_{H,ex}^3)(H_{ex}/H_{ex,i})^3 - c_j/(3K_{ex}m_{A,ex})\} \\ = (n_B/3m_{A,ex})(b_n - b_i) \\ = (n_C/3m_{A,ex})(c_i - c_n) \quad (23)$$

$$a_j = 3A_j/H_{in,0}, \quad b_j = B_j/B_0, \quad c_j = 3C_j/B_0, \quad y = A_{ex}/A_{ex,0}, \\ Bi = k_A R/D_{eB}, \quad m_{A,ex} = A_{ex,0}/B_0, \quad m_{A,in} = 3A_{in,0}/B_0, \\ m_{H,ex} = H_{ex,0}/B_0, \quad m_{H,in} = H_{in,0}/B_0, \quad n_B = k_B/k_A, \quad n_C = k_C/k_A, \\ n_f = k_f/k_A, \quad n_H = k_H/k_A, \quad q = Rk_r/R_\mu k_A, \quad r_{CB} = D_{eC}/D_{eB}, \\ s_j = S_j/4\pi R^2, \quad v_j = V_j/V_e, \quad \alpha = Rv_b/k_A V_T, \\ \kappa_{B,j} = k_{B,j}(R/D_{eB}), \quad \kappa_{C,j} = k_{C,j}(R/D_{eB}), \quad \theta = D_{eB}t/R^2 \quad (24)$$

It can be recognized from a comparison of these parameters with those in the previous model (10) that the present model is essentially the same as the previous model. In the present model, however, the method of division is more flexible, and the computation time is considerably

reduced. Furthermore, the nonideal behavior such as the swelling of the W/O emulsion can be more easily taken into account in this model.

If the values of 15 parameters ( $\alpha$ ,  $\phi$ ,  $\phi'$ ,  $Bi$ ,  $m_{A,ex}$ ,  $m_{A,in}$ ,  $m_{H,ex}$ ,  $m_{H,in}$ ,  $n_B$ ,  $n_C$ ,  $n_f$ ,  $n_H$ ,  $q$ ,  $K_{ex}$ ,  $r_{CB}$ ) are given, the basic equations can be numerically integrated. Here, the Runge-Kutta-Verner method was used.

## EXPERIMENTAL

The extractant PC-88A, kindly supplied by Daihachi Chemicals Ind. Co. Ltd., Japan, with a purity of 95%, was used without further purification. This extractant has been developed especially for the separation of cobalt(II) and nickel(II), and also for the separation of rare earth metals (13). It was reported that in comparison with di-2-ethylhexyl phosphoric acid, PC-88A is suitable to the extraction of heavy rare earth metals because the stripping is much easier compared to di-2-ethylhexyl phosphoric acid. The aqueous solutions of lanthanoids were prepared by dissolving their chloride salts in deionized water. Distribution ratios were measured by the conventional method. An organic solution and an aqueous solution, the ionic strength of which was adjusted to 0.1 mol/dm<sup>3</sup> by sodium chloride, were equilibrated at 298 K, and the resulting aqueous solution was analyzed. The feed concentrations of the metal ions were about 100 ppm, and the pH was adjusted by hydrochloric acid.

The experimental apparatus used for the extraction by liquid surfactant membranes was the same as reported in a previous paper (10). The W/O emulsion was formulated from the organic and aqueous solutions. The organic membrane phase consisted of Dispersol, a sort of kerosene supplied from Shell Chemical Co. Ltd., in which were dissolved PC-88A and Span 80, an emulsifier. The concentration of Span 80 was 5 vol%. The equal volumes of organic solution thus prepared and the aqueous solutions containing hydrochloric acid and lithium chloride, which was used as a tracer for measuring the membrane breakup, were sonicated for 2 min by an ultrasonic homogenizer. W/O emulsion (20 cm<sup>3</sup>) was dispersed in an agitation vessel containing 0.65 dm<sup>3</sup> of the feed solution. The stirring speed was 250 rpm, and the temperature was 298 K. The pH of the feed solution was adjusted by 0.3 mol/dm<sup>3</sup> formic acid-sodium formate buffer solution in the range of pH above 2.6 and by hydrochloric acid in the lower pH range. Samples were taken from the external phase, and the lanthanoid concentration was determined by the Arsenazo III method or flame emission spectrometry. The drop size distributions of W/O emulsion drop and the internal droplet were measured by the photographic and microscopic methods, respectively.

Unless otherwise stated, the concentration of hydrochloric acid in the internal aqueous phase was 1 mol/dm<sup>3</sup>.

## RESULTS AND DISCUSSION

### Extraction Equilibria

If Eq. (2) holds, the distribution ratio is expressed by

$$D = [\text{LnR}_3(\text{HR})]/[\text{Ln}^{3+}] = K_{ex}[(\text{HR})_2]/[\text{H}^+]^3 \quad (25)$$

Experiments were carried out under the condition of low loading ratio, i.e., the condition that  $[\text{LnR}_3(\text{HR})]$  was less than 5% of the total carrier concentration. Here, it was assumed that PC-88A exists as its dimer in Dispersol. Figure 2 shows the plot of  $D$  against pH. The slopes of these plots for all metals are approximately 3. It was found from the plot of  $D$  vs  $[(\text{HR})_2]$  at constant pH that  $D$  is approximately proportional to  $[(\text{HR})_2]^3$ .  $D$  was independent of the metal concentration. Thus, the extraction equilibria can be expressed by Eq. (2). The determined values of  $K_{ex}$  are shown in Table 1.

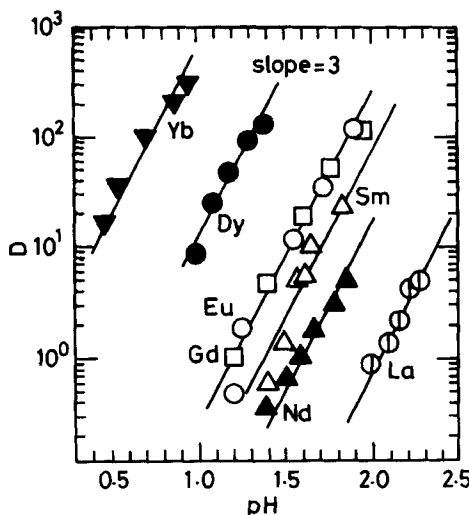


FIG. 2. Plot of  $D$  vs pH.  $[(\text{HR})_2] = 73.5 \text{ mol/m}^3$ ,  $[\text{Ln}^{3+}]_0 = 100 \text{ ppm}$ .

TABLE I  
Values of Parameters<sup>a</sup>

	La	Nd	Sm	Eu	Gd	Dy	Yb
$K_f^a$	0.002	0.03	0.15	0.30	0.60	25	1500
$k_f^b$	$5 \times 10^{-10}$	$2 \times 10^{-9}$	$8 \times 10^{-9}$	$5 \times 10^{-9c}$	$5 \times 10^{-8}$	$1 \times 10^{-7}$	$2 \times 10^{-6}$

<sup>a</sup> $k_A = 4 \times 10^{-5}$  m/s,  $k_B = 4 \times 10^{-5}$  m/s,  $D_{eB} = 1.5 \times 10^{-10}$  m<sup>2</sup>/s,  $R = 3 \times 10^{-4}$  m,  $R_u = 1 \times 10^{-6}$  m,  $r_{CB} = 0.52$ ,  $\alpha = 1.0 \times 10^{-6}$ .

<sup>b</sup>Unit is m/s.

<sup>c</sup>The value of  $k_f$  used in the simulation of the data in Fig. 9, and Figs. 12-14 is  $2 \times 10^{-8}$  m/s. This value is 4 times larger than that in this table. Both data are plotted in Fig. 7. The composition of Span 80 differs considerably from one lot to another, and the interfacial activity of Span 80 also differs depending on the lot. Since the reaction of lanthanoid ion and PC-88A occurs at the aqueous-organic interface, the rate is greatly influenced by the interfacial activity of Span 80. Span 80 of the same lot was not used in these two series of experiments. This may be the cause of the discrepancy in the value of  $k_f$ .

The effect of the addition of Span 80 on  $K_{ex}$  was investigated using W/O/W emulsion systems by means of the same technique employed in the extraction of phenol and cresol (14). However, a noticeable effect was not found in the concentration range of Span 80 below 5 vol%.

### Extraction by Liquid Surfactant Membranes

#### Comparison of the Extraction Rates of Lanthanoid Ions by Liquid Surfactant Membranes

The comparison of the extraction rates of various lanthanoid ions by liquid surfactant membranes at pH = 2.3 is shown in Fig. 3. The order of the extraction rate is essentially the same as the order of  $K_{ex}$ , and the metal of higher atomic number is extracted more rapidly.

In the conventional extraction of  $\text{Yb}^{3+}$  carried out at high loading ratio, the aggregates of metal-carrier complexes were formed, and the organic phase set to gel. However, in the case of liquid surfactant membranes, the formation of such aggregates was suppressed because both the extraction and the stripping occurred simultaneously on both side of the membranes. Thus, the liquid surfactant membrane is recommended in such systems.

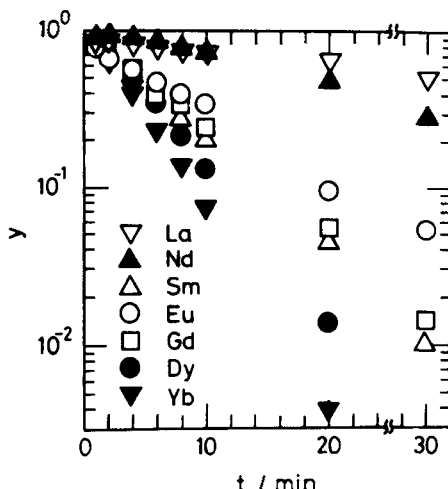


Fig. 3. Extraction of various lanthanoids by liquid surfactant membranes.  $[\text{Ln}^{3+}]_{ex,0} = 200$  ppm, pH = 2.3,  $[(\text{HR})_2]_0 = 73.5 \text{ mol/m}^3$ ,  $[\text{H}^+]_{in,0} = 1000 \text{ mol/m}^3$ .

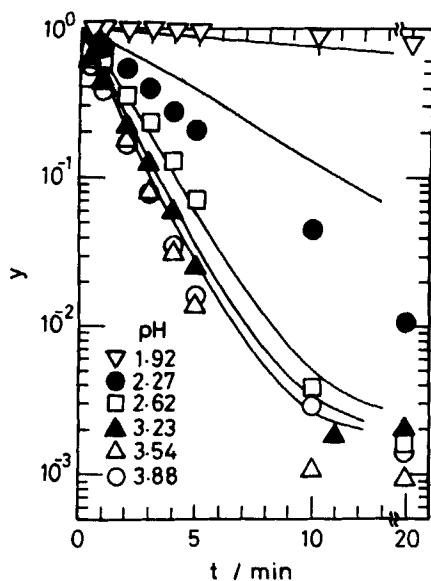


FIG. 4. Effect of hydrogen ion concentration on the extraction rate of samarium(III).  $[\text{Sm}^{3+}]_{\text{ex},0} = 1.32 \text{ mol/m}^3$ ,  $[(\text{HR})_2]_0 = 73.5 \text{ mol/m}^3$ ,  $[\text{H}^+]_{\text{in},0} = 1000 \text{ mol/m}^3$ .

### Determination of the Rate Constant of the Interfacial Reaction

The effect of pH on the extraction rate of samarium(III) is shown in Fig. 4. The extraction rate increases with pH. However, in the range of high pH, further increase in pH does not increase the extraction rate. Similar behavior was observed in the extraction of copper(II) (10). This can be explained as follows. When the pH is low, both the interfacial reaction rate and the distribution ratio are low, and the extraction rate decreases with a decrease in pH. On the other hand, when pH is high and the metal concentration is low, both the interfacial reaction rate and the distribution ratio are high. Therefore, the resistances of the reaction and the diffusion of the complex in the membrane can be neglected while the diffusion of  $\text{Sm}^{3+}$  in the stagnant film of the external aqueous phase is rate-determining. Thus, the extraction rate is not influenced by pH in the range of high pH. The value of  $k_A$  was obtained from Eq. (26) by using the data in this region.

$$\ln([\text{Sm}]_{\text{ex}}/[\text{Sm}]_{\text{ex},0}) = \ln y = -(k_A S_T / V_{\text{ex}})t = -(3k_A V_e / R V_{\text{ex}})t \quad (26)$$

To examine whether the rate of the interfacial reaction follows Eq. (3), a

series of experiments on the extraction of europium was carried out under the condition of reaction rate-controlling. Here, it was assumed that at low pH the rate-determining step is the interfacial reaction. The rate of the reverse reaction could be neglected under the experimental condition. Then, the relation of  $y$  ( $= [Eu]_{ex}/[Eu]_{ex,0}$ ) vs  $t$  at low pH is given by

$$\ln y = -kt \quad (27)$$

$$k = (k_f B_0^3 / H_{ex}^3) (S_T / V_{ex}) = (k_f B_0^3 / H_{ex}^3) (3V_e / RV_{ex}) \quad (28)$$

It was found that the plots of  $\ln y$  vs  $t$  gave straight lines, and the values of  $k$  were calculated from the slopes. As shown in Fig. 5, the plot of  $k$  vs hydrogen ion concentration at constant carrier concentration gives a straight line with a slope of  $-3$ . It was also found that the slope of the plot of  $k$  vs carrier concentration was 3 as shown in Fig. 6. These results are in

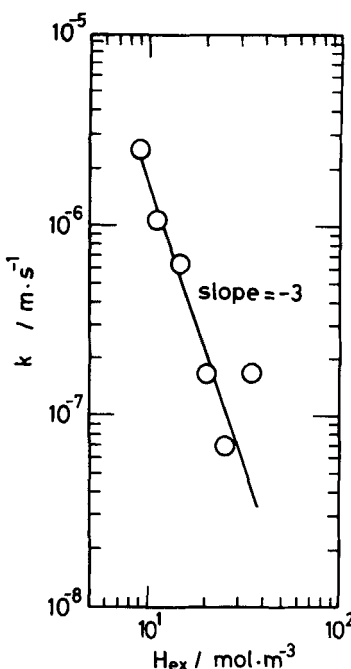


FIG. 5. Plot of  $k$  vs  $H_{ex}$ .  $[\text{Eu}^{3+}]_{ex,0} = 1.32 \text{ mol/m}^3$ ,  $[(\text{HR})_2]_0 = 73.5 \text{ mol/m}^3$ ,  $[\text{H}^+]_{in,0} = 1000 \text{ mol/m}^3$ .

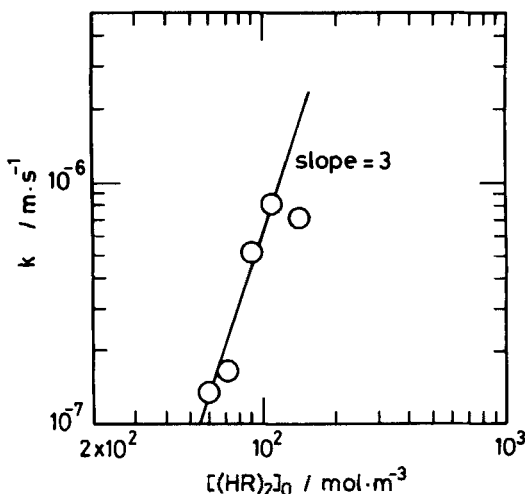


FIG. 6. Plot of  $k$  vs  $[(HR)_2]_0$ .  $[\text{Eu}^{3+}]_{ex,0} = 1.32 \text{ mol/m}^3$ ,  $\text{pH} = 2$ ,  $[\text{H}^+]_{in,0} = 1000 \text{ mol/m}^3$ .

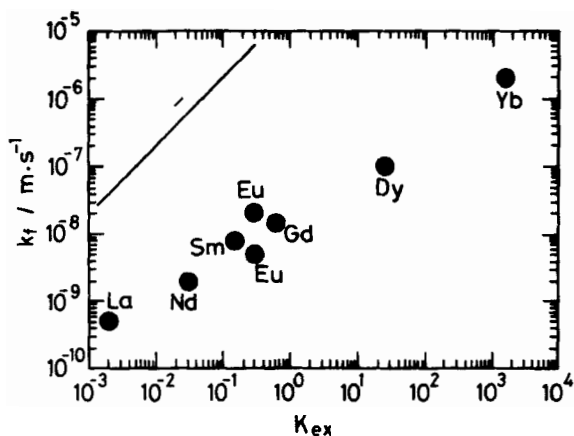
agreement with the proposed rate equation. The values of  $k_f$  thus obtained are shown in Table 1.

The plot of  $k_f$  vs  $K_{ex}$  is shown in Fig. 7. The slope is approximately 0.67, and  $k_f$  for  $\text{Yb}^{3+}$  is about three orders of magnitude higher than  $k_f$  for  $\text{La}^{3+}$ .

On the other hand, if it is assumed that even at low pH, the interfacial reaction is so fast that the chemical equilibrium holds at the interface between the external aqueous phase and the W/O emulsion drop, and also that the diffusion of the complex through the peripheral oil layer around the W/O emulsion drop is rate controlling, the following rate equation can be obtained which shows the same concentration dependencies as Eq. (3).

$$r_f = k_c C_i = k_c K_{ex} A_{ex,i} B_i^3 / H_{ex,i}^3 = k_c K_{ex} A_{ex} B_0^3 / H_{ex}^3 \quad (29)$$

Here,  $k_c$  is the mass transfer coefficient of the complex through the peripheral oil layer. From the comparison of Eq. (29) with Eq. (3), it is recognized that  $k_f$  in Eq. (3) corresponds to  $k_c K_{ex}$  in Eq. (29). As will be shown later, the value of  $k_c$  was determined as  $2.1 \times 10^{-5} \text{ m/s}$ . The solid line in Fig. 7 shows the relation of  $k_f = k_c K_{ex}$ . The large discrepancy between the data and the solid line indicates that the assumption of chemical equilibrium at the interface is not reasonable. Thus, it may be

FIG. 7. Plot of  $k_f$  vs  $K_{ex}$ .

considered that  $k_f$  shown in Fig. 7 is the interfacial reaction rate constant rather than  $k_C K_{ex}$ . However, if the interfacial reaction follows the Eigen mechanism (15), the values of  $k_f$  are roughly of the same order of magnitude for these lanthanoids. Further investigation is needed to interpret the behavior shown in Fig. 7.

It had been found from an experiment using a Lewis-type transfer cell that the extraction rate of copper(II) with SME529 was remarkably reduced by the addition of Span 80 (16). A similar experiment was carried out on the extraction of  $\text{Eu}^{3+}$ . The organic phase containing PC-88A and



varying amounts of Span 80 was contacted with an aqueous solution of europium(III). The details of the experimental apparatus and the procedure are described elsewhere (17). As shown in Fig. 8, the extraction rate was considerably decreased by the presence of a very small amount of Span 80.

### Effect of Experimental Condition on the Extraction Rate

Figure 9 shows the effect of pH on the extraction rate of  $\text{Eu}^{3+}$ . The volume ratio of the W/O emulsion to the external feed solution was as low as 1/32. In the range of pH above 2.95, the extraction rate is not influenced by pH as in the case of the extraction of  $\text{Sm}^{3+}$ . It should be noted that in spite of a very low volume ratio, 99% of europium was extracted within 10 min, and that the ratio of the concentration of  $\text{Eu}^{3+}$  in the internal aqueous phase to that in the external feed solution reached about 50,000 in 20 min.

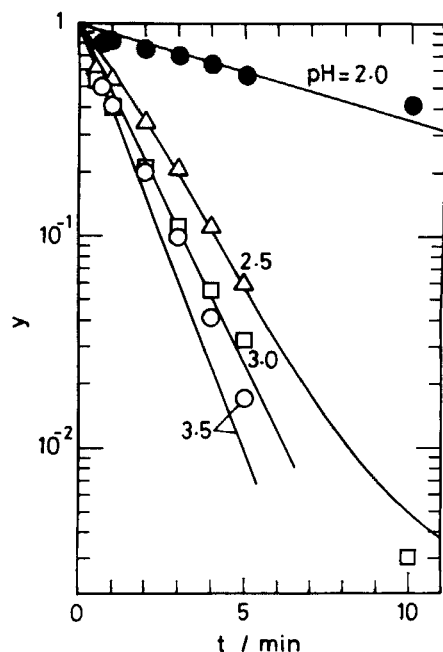


FIG. 9. Effect of pH on the extraction rate of europium(III).  $[\text{Eu}^{3+}]_{\text{ex},0} = 1.32 \text{ mol/m}^3$ ,  $[(\text{HR})_2]_0 = 73.5 \text{ mol/m}^3$ ,  $[\text{H}^+]_{\text{in},0} = 1000 \text{ mol/m}^3$ .

The effects of pH on the extraction rates of  $\text{La}^{3+}$  and  $\text{Nd}^{3+}$  are shown in Figs. 10 and 11, respectively. In the extraction of  $\text{La}^{3+}$ , the critical pH above which the extraction rate becomes almost constant is considerably higher than in the extraction of  $\text{Eu}^{3+}$ .

Figure 12 shows the effect of europium concentration in the feed solution. It is seen that the degree of the extraction decreases with the increase in  $[\text{Eu}^{3+}]_{\text{ex},0}$ . This is explained as follows. When  $[\text{Eu}^{3+}]_{\text{ex},0}$  is high, the internal droplets in the peripheral region of the W/O emulsion drop are more rapidly saturated, and the rate is controlled by internal diffusion, i.e., by the diffusion in the W/O emulsion drop, and  $-dy/dt$  becomes low. On the other hand, when  $[\text{Eu}^{3+}]_{\text{ex},0}$  is low,  $-dy/dt$  becomes high because the rate is controlled by external diffusion, i.e., diffusion of  $\text{Eu}^{3+}$  in the stagnant film outside the W/O emulsion drop, and other resistances can be ignored (10).

Figure 13 shows the effect of the carrier concentration on the extraction rate of  $\text{Eu}^{3+}$ . The rate increases with increasing carrier concentration because both the interfacial reaction rate and the distribution ratio increase. However, in the concentration range above 28 mol/m<sup>3</sup>, the rate is independent of the carrier concentration since the external diffusion is

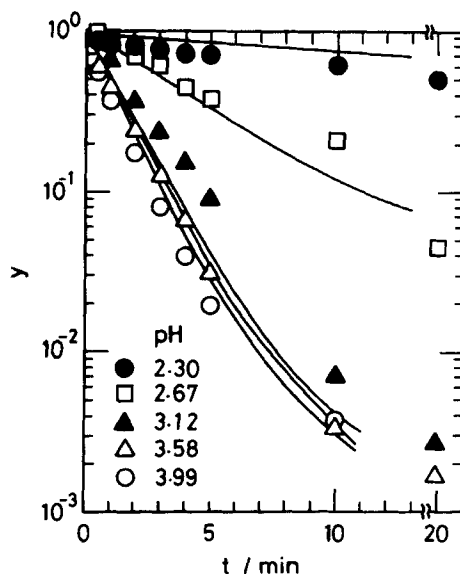


FIG. 10. Effect of pH on the extraction rate of lanthanum(III).  $[\text{La}^{3+}]_{\text{ex},0} = 1.44 \text{ mol/m}^3$ ,  $(\text{HR})_2|_0 = 73.5 \text{ mol/m}^3$ ,  $[\text{H}^+]_{\text{in},0} = 1000 \text{ mol/m}^3$ .

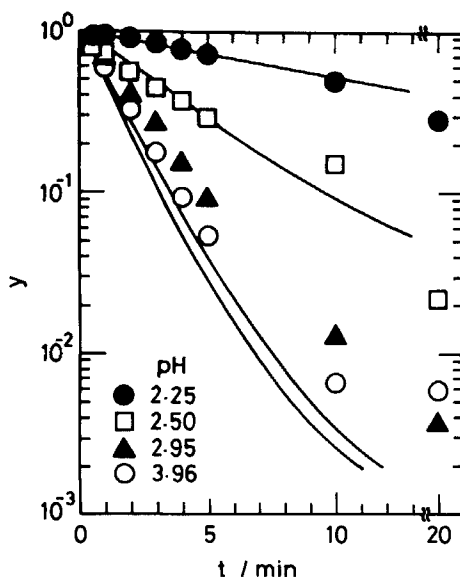


FIG. 11. Effect of pH on the extraction rate of neodymium(III).  $[Nd^{3+}]_{ex,0} = 1.39 \text{ mol/m}^3$ ,  $[(HR)_2]_0 = 73.5 \text{ mol/m}^3$ ,  $[H^+]_{in,0} = 1000 \text{ mol/m}^3$ .

rate controlling in this concentration range. Thus, it should be emphasized that external diffusion is very important when the extraction rate is fast and the metal concentration is low.

The effect of hydrochloric acid concentration in the internal aqueous phase is shown in Fig. 14. It is seen that when  $[Eu^{3+}]_{ex,0}$  is low, the effect of  $[HCl]_{in,0}$  is not observed because the external diffusion is rate controlling. On the other hand, when  $[Eu^{3+}]_{ex,0}$  is high, the internal diffusion becomes important, and the rate increases with increasing  $[HCl]_{in,0}$  because the capacity of the internal aqueous phase as a sink for  $Eu^{3+}$  increases and the resistance of the internal diffusion decreases.

### Comparison of the Experimental Data with the Computed Results

The parameters involved in the multilayer shell model were estimated as follows. The value of  $k_A$  was estimated by Eq. (29) by using the data obtained under the condition of external diffusion control. The mass transfer resistance of  $H^+$  in the external phase is important only when the extraction rate is fast, i.e., at high pH. However, in the experiment at high

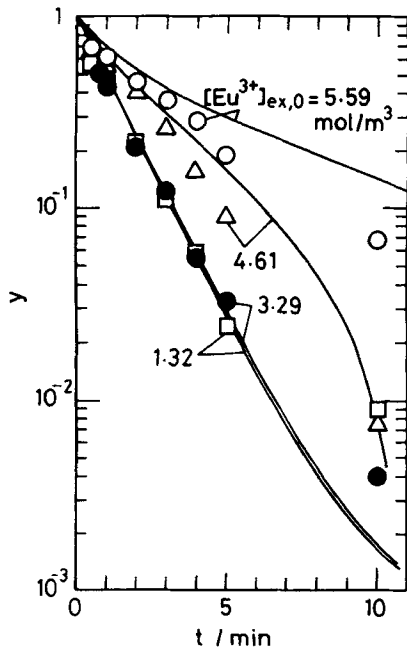


FIG. 12. Effect of europium concentration on the extraction rate.  $\text{pH} = 2$ ,  $[(\text{HR})_2]_0 = 73.5 \text{ mol/m}^3$ ,  $[\text{H}^+]_{in,0} = 1000 \text{ mol/m}^3$ .

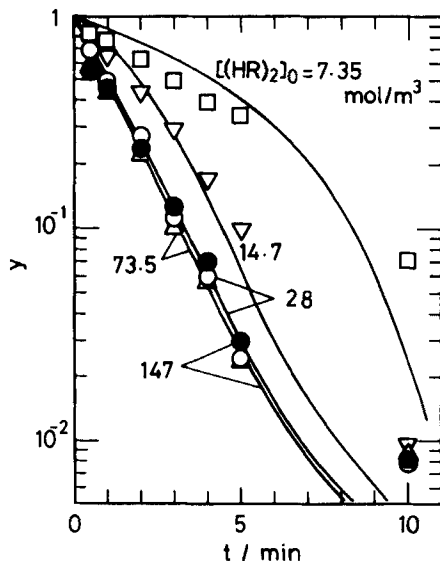


FIG. 13. Effect of the carrier concentration on the extraction rate of europium(III).  $[\text{Eu}^{3+}]_{ex,0} = 1.36 \text{ mol/m}^3$ ,  $\text{pH} = 2$ ,  $[\text{H}^+]_{in,0} = 1000 \text{ mol/m}^3$ .

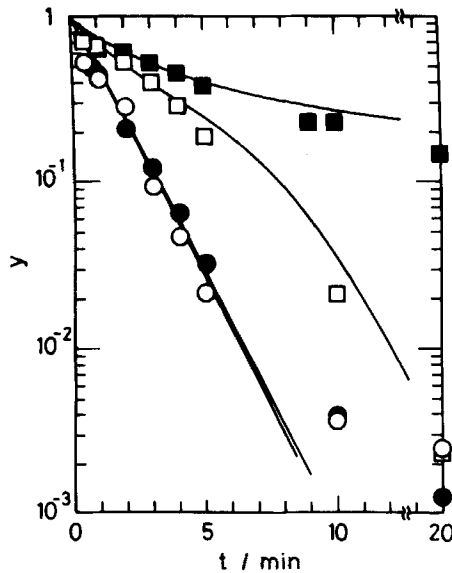


FIG. 14. Effect of hydrochloric acid concentration in the external phase on the extraction rate of europium(III). pH = 2.

	■	□	●	○
$[\text{Eu}^{3+}]_{\text{ex},0}$ (mol/m <sup>3</sup> )	6.58	6.58	3.29	3.29
$[\text{H}^+]_{\text{in},0}$ (mol/m <sup>3</sup> )	1000	1500	1000	1500

pH, buffer solutions were used. Therefore, this resistance was not considered.  $D_{eB}$  and  $k_B$  were determined so that the computed results could be compared with the experimental data. Here, it was assumed that the equations  $D_C/D_B = D_{eC}/D_{eB} = k_C/k_B$ , and  $D_C/D_B = \{(\text{molar volume of } B)/(\text{molar volume of } C)\}^{0.6}$  (18) hold. The estimated values are shown in Table 1. The ratio of  $D_{eB}$  to  $D_B$ , the bulk diffusivity of the carrier, is 0.75. This value is considerably higher than 0.24 which was obtained in the extraction of copper by liquid surfactant membranes (10). It was observed that the W/O emulsion used in the present experiment was less viscous than those in the copper extraction. Thus, some convection in the W/O emulsion drop may contribute to the higher value of  $D_{eB}/D_B$ .

The solid lines in Fig. 4 and Figs. 9-14 are computed results. It is seen that the experimental data could be satisfactorily simulated by the proposed permeation model. It was found from the computed concentration profiles in the W/O emulsion drop that chemical equilibrium is established between the oil membrane phase and the internal aqueous phase.

## CONCLUSION

Extractions of  $\text{La}^{3+}$ ,  $\text{Nd}^{3+}$ ,  $\text{Sm}^{3+}$ ,  $\text{Eu}^{3+}$ ,  $\text{Gd}^{3+}$ ,  $\text{Dy}^{3+}$ , and  $\text{Yb}^{3+}$  by liquid surfactant membranes were carried out using 2-ethylhexyl phosphonic acid mono-2-ethylhexyl ester as a carrier. It was found that the kinetics of the interfacial reaction follow Eq. (3), and also that a correlation holds between the rate constant and the extraction constant. The effects of the experimental conditions on the extraction rate were satisfactorily simulated by the proposed permeation model, i.e., the multilayer shell model.

## SYMBOLS

$A$	concentration of $\text{Ln}^{3+}$ ( $\text{mol}/\text{m}^3$ )
$A_j$	concentration of $\text{Ln}^{3+}$ in internal aqueous phase of $j$ th shell ( $\text{mol}/\text{m}^3$ )
$B$	concentration of carrier ( $\text{mol}/\text{m}^3$ )
$b$	$B/B_0$
$Bi$	Biot number ( $= k_A R/D_{eB}$ )
$C$	concentration of complex ( $\text{mol}/\text{m}^3$ )
$c$	$3C/B_0$
$D$	molecular diffusivity ( $\text{m}^2/\text{s}$ )
$D_e$	effective diffusivity ( $\text{m}^2/\text{s}$ )
$H$	concentration of $\text{H}^+$ ( $\text{mol}/\text{m}^3$ )
$H_j$	concentration of $\text{H}^+$ in internal aqueous phase of $j$ th shell ( $\text{mol}/\text{m}^3$ )
$K_{ex}$	extraction constant
$k$	quantity defined by Eq. (28) ( $1/\text{s}$ )
$k_A, k_H$	mass transfer coefficients of $\text{Ln}^{3+}$ and $\text{H}^+$ through external aqueous stagnant film, respectively ( $\text{m}/\text{s}$ )
$k_B, k_C$	mass transfer coefficients of carrier and complex through the peripheral oil layer of W/O emulsion ( $\text{m}/\text{s}$ )
$k_f, k_r$	forward and reverse reaction rate constants, respectively, ( $\text{m}/\text{s}$ )
$k_{J,j}$	mass transfer coefficient between $j$ th and $(j + 1)$ th shell ( $J = B, C$ ) ( $\text{m}/\text{s}$ )
$m$	initial concentration ratio defined by Eq. (24)
$n$	number of division of W/O emulsion drop
$n_J$	$k_J/k_A$ ( $J = B, C, H$ , and $f$ )
$q$	$Rk_r/R_A k_A$
$R$	radius of W/O emulsion drop ( $\text{m}$ )

$R_p$	radius of internal droplet (m)
$r$	rate of interfacial reaction (mol/m <sup>2</sup> · s)
$r_{CB}$	$D_C/D_B$ or $D_{eC}/D_{eB}$
$S_j$	interfacial area between $j$ th and $(j + 1)$ th shell (m <sup>2</sup> )
$S_T$	total surface area of W/O emulsion drops (m <sup>2</sup> )
$S_j$	$S_j/(4\pi R^2)$
$t$	time (s)
$V_e$	total volume of W/O emulsion (m <sup>3</sup> )
$V_{ex}$	volume of external aqueous phase (m <sup>3</sup> )
$V_T$	total volume ( $= V_e + V_{ex}$ ) (m <sup>3</sup> )
$v_b$	volumetric rate of leakage of internal phase to external phase due to membrane breakup (m <sup>3</sup> /s)
$v_j$	$V_j/V_e$
$w_j$	$3A_j/H_{in,0}$
$y$	$A_{ex}/A_{ex,0}$

### Subscripts

0	initial value
$A$	lanthanoid
$B$	carrier
$b$	bulk liquid
$C$	complex
$H$	hydrogen ion
$e$	W/O emulsion
$ex$	external aqueous phase
$f$	forward reaction
$i$	interface between external aqueous phase and W/O emulsion drop
$in$	internal aqueous phase
$j$	$j$ th shell
$r$	reverse reaction

### Greeks

$\alpha$	$Rv_b/k_A V_T$
$\phi$	volume fraction of internal aqueous phase in W/O emulsion ( $= V_{in}/V_e$ )
$\phi'$	volume fraction of W/O emulsion in W/O/W multiple emulsion ( $= V_e/V_T$ )
$\theta$	$D_{ebt}/R^2$

## Acknowledgments

This work was supported by a Grant-in-Aid for the Special Research Project on Environmental Science from the Ministry of Education, Culture and Science, Japan, in 1983 (No. 58030045), and by the Asahi Glass Foundation for Industrial Technology. We thank the Shell Chemical Co Ltd. for supplying Dispersol. We also thank Daihachi Chemicals Ind. Co. Ltd., Japan, for supplying PC-88A.

## REFERENCES

1. R. Marr and A. Kopp, *Chem.-Ing.-Tech.*, **52**, 399 (1980).
2. N. N. Li, R. P. Cahn, D. Naden, and R. W. M. Lai, *Hydrometallurgy*, **9**, 277 (1983).
3. M. Prötsch and R. Marr, *Proc. ISEC '83*, p. 66 (1983).
4. E. J. Fuller and N. N. Li, *J. Membr. Sci.*, **18**, 251 (1984).
5. T. Kitagawa, Y. Nishikawa, J. W. Frankenfeld, and N. N. Li, *Environ. Sci. Technol.*, **11**, 602 (1977).
6. J. Strzelbicki and W. Charewicz, *Hydrometallurgy*, **5**, 243 (1980).
7. H. C. Hayworth, W. S. Ho, W. A. Burns Jr., and N. N. Li, *Sep. Sci. Technol.*, **18**, 493 (1983).
8. C. Jiang, J. Yu, and Y. Zhu, *J. Chem. Ind. Chem. Eng. (China)*, p. 225 (1982).
9. Y. Zhu, C. Jiang, S. Wang, Z. Lui, and J. Yu, *Proc. ISEC '83*, p. 58 (1983).
10. M. Teramoto, T. Sakai, K. Yanagawa, and Y. Miyake, *Sep. Sci. Technol.*, **18**, 735 (1983).
11. M. Teramoto, T. Sakai, K. Yanagawa, and Y. Miyake, *Ibid.*, **18**, 985 (1983).
12. E. Ma, X. Yan, S. Wang, H. Long, and C. Yuan, *Proc. ISEC '80*, p. 80 (1980).
13. A. Fujimoto, I. Miura, and K. Noguchi, U.S. Patent 4,196,076 (1980).
14. M. Teramoto, H. Takihana, M. Shibutani, T. Yuasa, and N. Hara, *Sep. Sci. Technol.*, **18**, 397 (1983).
15. M. Eigen and K. Tamm, *Z. Elektrochem.*, **66**, 107 (1962).
16. M. Teramoto, Y. Miyake, and N. Tokuda, Unpublished Work.
17. Y. Miyake, Y. Takenoshita, and M. Teramoto, *J. Chem. Eng. Jpn.*, **16**, 203 (1981).
18. C. R. Wilke and P. Chang, *AIChE J.*, **1**, 264 (1955).

Received by editor July 15, 1985